



Bio-inspired designing strategy and properties of energetic crystals@ (CNFs@PDA) composites

Ling Chen · Derong Meng · Jianwei Zhang ·
Xiang Cao · Fengqiang Nan · Xin Liao ·
Weidong He

Received: 18 February 2023 / Accepted: 13 June 2023 / Published online: 27 July 2023
© The Author(s), under exclusive licence to Springer Nature B.V. 2023

Abstract The inherent high sensitivity and polymorphs phase transition of 1,3,5-trinitroperhydro-1,3,5-triazine (RDX), 1,3,5,7-tetranitro-1,3,5,7-tetrazocane (HMX) and 2,4,6,8,10,12-hexanitro-2,4,6,8,10,12-hexaazaisowurtzitane (CL-20) have impeded their extensive practical applications in propellants. Recently, cellulose nanofibers (CNFs) have attracted an intense attention due to its biodegradable, outstanding mechanical properties, and tunable surface physicochemical, thereby possessing promising application in energetic materials. However, the poor hydrophobicity and dispersion of CNFs easily agglomerate to units, which may encounter low-utilization of CNFs. Inspired by the strong chemical adhesion properties of mussels, a facile and

noncovalent in-situ polymerization of dopamine was introduced to modify CNFs through a simple immersion method. Then, utilizing the as-prepared CNFs@PDA (polydopamine) to modify the energetic crystals via a brief and safe water suspension method. The in-depth characterizations of the obtained energetic crystal@(CNFs@PDA) composites demonstrate that CNFs were coated with a dense coating PDA, wherein CNFs@PDA deposit uniformly on the surfaces of energetic crystals, and the dispersibility of CNFs was improved remarkably. In addition, the thermal stability was obviously improved, whose phase transition temperature of HMX and CL-20 in the increased $\beta \rightarrow \delta$ and $\epsilon \rightarrow \gamma$ from 184.1 to 206.9 °C and from 162.7 to 182.2 °C, respectively. The sensitivity of composites was also significantly decreased compared with original energetic crystals. Hence, this construction strategy of energetic crystal@(CNFs@PDA) composites provides a promising method for the modification of energetic crystals and application potential propellants.

Supplementary Information The online version contains supplementary material available at <https://doi.org/10.1007/s10570-023-05324-3>.

L. Chen · D. Meng · J. Zhang · X. Cao · F. Nan (✉) ·
X. Liao · W. He (✉)
School of Chemistry and Chemical Engineering, Nanjing
University of Science and Technology, Nanjing 210094,
Jiangsu, China
e-mail: nanfq@163.com

W. He
e-mail: hewedong@njust.edu.cn

L. Chen · D. Meng · J. Zhang · X. Cao · F. Nan · X. Liao ·
W. He
Key Laboratory of Special Energy Materials, Ministry
of Education, Nanjing 210094, Jiangsu, China

Keywords Energetic crystal · CNFs@PDA · Core-shell structure · Stability · Sensitivity

Introduction

In the domain of energetic materials (EMs), the high-energy and insensitive EMs plays as an important direction needing to be developed (Xie et al.

2018). Therein, nitramine explosive crystals like hexahydro-1,3,5-trinitro-1,3,5-triazine (RDX), 1,3,5,7-tetranitro-1,3,5,7-tetrazocane (HMX), and 2,4,6,8,10,12-hexanitro-2,4,6,8,10,12-hexaazaisowurtzitane (CL-20) usually act as the mainly solid components to enhance the energy performance of propellants (Chen et al. 2021a). Whereas, high-energy explosives usually feature high mechanical sensitivities (*e.g.*, impact and friction), thus causing accidental combustion or explosion and significant economic losses, even resulting in casualties during their process of development, production, storage, transportation and application when encounter external energy stimulation (Chen et al. 2021b). Additionally, the polymorphic phase transition of HMX (α , β , γ , σ) and CL-20 (α , β , γ , δ , ϵ) may occur once encountering external stimuli, and lead to non-negligible restriction and potential dangers, which is another issue need to be addressed (Cady et al. 1963; Shen et al. 2014). Moreover, the introduction of a mass of high-energy solid fillers may also weaken the mechanical properties of propellants (Shen et al. 2019, 2020; Wang et al. 2020b). Therefore, addressing the balance between the high-energy and high-safety of EMs remains a highly challenging task that is what the world scientist common research.

Over the past decades, numerous strategies have been implemented to realize this balance, such as the superfine smash technology, surface coating method (Shu et al. 2015; Yuan and Xiao-Qing 2011), recrystallization (Chauhan et al. 2021; Guillevic et al. 2020; Liu et al. 2019), co-crystallization (Sinditskii et al. 2020; Song et al. 2018; Zhang et al. 2018), and so forth. Among these mentioned methods or technologies, the surface coating method has been proved to be the best and the most widely used ones, attributing to their safer and cost-effective operations with well-controlled procedures, that endow products with tunable performances (Huang et al. 2021). Up till now, surface coating method has been manifested to be an effective way to enhance the thermal stability and improve the safety performance of EMs with insensitive materials modifying the surface of energetic crystal (Doukkali et al. 2017). More important, choosing suitable insensitive agents is also another essential factor to satisfy the comprehensive performances of Ems (Yang et al. 2015). Hence, the development of novel insensitive, high-strengthen and high-energy EMs could be obtained through coating material

innovation (Lin et al. 2018). In previous work, carbon materials (Wang et al. 2018; Ye et al. 2018), organic synthetic material (Jia et al. 2019, 2018; Wang et al. 2016; Yang et al. 2015; Zhang et al. 2019a, 2019b), biological materials (Chen et al. 2021c; Gong et al. 2017; Lin et al. 2019), Inorganic metals or their oxides and so forth (Aduiev et al. 2021; Mao et al. 2018; Zeng et al. 2021; Zhou et al. 2019) were utilized to modify the surface of energetic crystals and obtained typical core-shell structure energetic composites with improved thermal stability and insensitivity. Recently, the emerging naturally derived cellulose nanofibers (CNFs) have absorbed an increasing attention on account of their biodegradable, high strength, high surface area, and tunable surface chemistry (De France et al. 2021). Therefore, CNFs could act as functional reinforce materials, particularly the high strength and tunable surface chemistry, to provide application potential to the improvement mechanical performance of EMs (Zhang et al. 2016). Nevertheless, the inherent strong hydrophilicity and water absorption properties of CNFs may result in poor dispersion and easily agglomerate to units with low-utilization in the actual applications (Wang et al. 2020a). Hence, improving the dispersibility of CNFs and impeding the agglomeration phenomenon of CNFs are of immense significance to widen the actual application in many kinds of fields (Huang et al. 2020).

Inspired by the adhesive nature structure of catechol and amines in mussel-adhesive proteins, polydopamine (PDA) (molecular structure shown in Fig. 1) has attracted great research interests and became a unique “bio-glue” since its strong and universal adhesion ability (He et al. 2017; Lin et al. 2018). The use of dopamine solutions as dip-coating through the oxidation-polymerization of monomers has provided a simple and versatile method for modifying surfaces of solid materials, and led to the development of bio-inspired PDA for the successful modification of various substrates, including metals, metals with native oxide surface, semiconductors, ceramics, carbon materials, and synthetic polymers (Lee et al. 2007; Maerten et al. 2015). In addition, the PDA-mediated chemistry also provides a general method for the fabrication of numerous multifunctional substrates with specific properties (Dreyer et al. 2013; Liu et al. 2014).

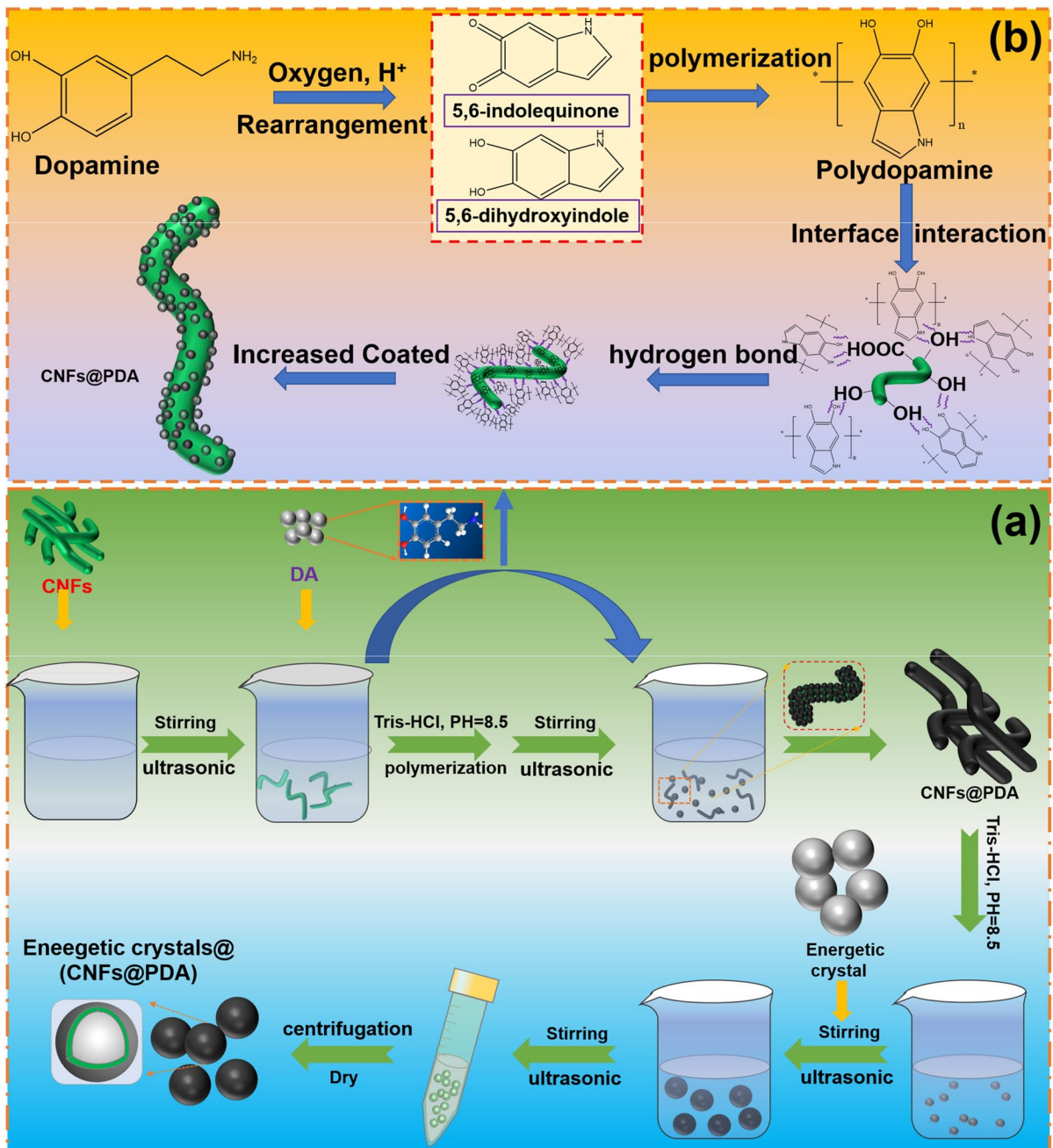


Fig. 1 The preparation process of CNFs@PDA coated nitramine explosive composites (a) and the coating process of CNFs@PDA (b)

Herein, in order to reduce the sensitivity of nitramine explosive crystal as well as maintaining favorable thermal stability, mussel-inspired by the strong adhesion ability of PDA, this study intends to firstly prepare CNFs@PDA composite materials

through an in-situ polymerization of dopamine to improve the dispersibility and interfacial interaction of CNFs. After then, the as-prepared CNFs@PDA is utilized to modify the surface of energetic crystal via a facile ultrasonic method and a simple water

suspension method, respectively. The characterizations of SEM, XRD, FT-IR, Raman are employed to study the stability of structure for samples, while the TG-DSC analysis is constructed to probe the thermal stability and decomposition behavior of samples. Finally, to investigate the safety performance of samples, the impact, friction and electrostatic spark sensitivity of sample are carried out. Meanwhile, the desensitization mechanism of energetic crystals modified by CNFs@PDA is discussed.

Experimental section

Materials

RDX (purity 99%), HMX (purity 97%), and CL-20 (purity 99%) were provided by Liaoning Qingyang Chemical Co., Ltd.; The concentration 5 wt% of CNFs is supplied by Beijing Institute of Technology (BIT). Dopamine hydrochloride and (hydroxymethyl)-aminomethane (Tris) were provided by Sigma-Aldrich and used as received. The deionized water is home-made.

Sample preparation

The preparation scheme of energetic composites is displayed in Fig. 1. The process of coating is performed typically as follows:

Firstly, the raw CNF suspension with concentration of about 5 wt% was diluted by 30 mL tris-solution into concentration of about 1.00 wt% with constant magnetic stirring (600 rpm·min⁻¹) to obtain homogeneously CNF suspension solutions for 15 min and ultrasonic for 20 min. Then, the 150 mg DA was added into above mentioned CNF suspension with constant magnetic stirring about 6 h and 20 ultrasonic for 20 min. Then, the energetic crystal RDX, HMX and CL-20 was added into the CNFs@PDA solution for 6 h, 12 h and 24 h. After then, the obtained solutions were separated by centrifugation and rinsed with large quantity of deionized water several times to remove excessive PDA. At last, the filtered products were dried in vacuo at 50 °C for 24 h. To further investigate the addition of CNFs@PDA content on the performance of energetic crystals, the two times and three times of CNFs@PDA content were prepared and used to modify the energetic crystals as the

above-mentioned process. These as-prepared samples were labelled as RDX@(CNFs@PDA)-6 h, RDX@(CNFs@PDA)-12 h, RDX@(CNFs@PDA)-24 h, RDX@(CNFs@PDA)_{1,2}-12 h, and RDX@(CNFs@PDA)_{1,3}-12 h, the same to that of HMX and CL-20.

Characterization

The morphological observation of these obtained samples was conducted by a field-emission scanning electron microscope (FESEM, FEI400, Hitachi Co., Ltd. Japan). The structure was detected by X-ray diffraction (XRD) analysis (Bruker D8 Advance, Germany), and the diffractometer uses Cu K α radiation under the conditions of 40 kV and 40 mA, while the scanning range for 2 θ is from 5 to 60° at the rate of 0.03°/0.1 s. Fourier transform infrared (FT-IR) spectroscopy (Nicolet iS10, Thermo Scientific, USA) was performed to analyze the organofunctional groups of the composites. To further investigate the structure and distribution of these samples and the disordering degree, Raman microscopy analysis using a confocal Raman spectrometer (Renishaw inVia-2JGY39) and groups mapping analysis were also conducted under the condition of 532 nm excitation. Notably, to prevent the decomposition or ablation phenomenon of the EMs due to the strong laser exposure, the laser beam was set on the as-prepared sample surface with a 50 \times objective for an exposure time of 5 s, at a low laser power of 10% in each time. Thermal decomposition properties were analyzed by differential scanning calorimetry (DSC, TA Instruments SDT 600). The samples were heated at range temperature of 100 to 350 °C with heating rates of 10 °C·min⁻¹, under a nitrogen (N₂) atmosphere at about 40 mL·min⁻¹ flow rate. In addition, Thermogravimetry (TG, STA 8000 instruments) has also been carried out to probe the thermal property of composites at heating rate of 10 °C·min⁻¹ from 100 to 400 °C with N₂ about 20 mL·min⁻¹. The mass of the tested samples of about 1.5 mg was added to an Al₂O₃ crucible.

For the sensitivity test of samples, the impact sensitivity was carried out by the principle of GJB772A-97 with a fall hammer of OZM research BAM Fall hammer device, and 25 samples with mass of 50 \pm 1 mg were tested by drop weight about 5 kg, room temperature of 19 °C, and relative humidity of 16%. The special height (H_{50}) representing the drop height of 50% explosion

probability to illustrate the results. The physical pictures of BAM Fall hammer device and the schematic of the impact sensitivity assembly are displayed in Figure S1 and Figure S2.

In terms of the friction sensitivity, which was tested by using MGY-1 friction instruments based on the rule of GJB 602.1. During each determination, 25 samples were tested and the explosion probability (P , %) was obtained. The physical picture of the instrument and the simple diagram illustration was shown in Figure S3.

The electrostatic spark sensitivity was measured by utilizing an instrument of OZM research Xspark10 tester. The samples were placed between two electrodes discharge with 0.25 mm and initiated by a set voltage. The electrostatic spark energy (E_{50}) was calculated according to equation:

$$E_{50} = \frac{1}{2}CU^2$$

where the C is capacitance and U is voltage. The E_{50} was adjusted by set the value of C and U .

The physical photos of electrostatic discharge sensitivity test device and the scheme of the static spark gap assembly were presented in Figure S4 and Figure S5.

Results and discussion

Morphologies

The morphologies of raw RDX, HMX, CL-20 and CNFs@PDA coated energetic composites were obtained by SEM, as displayed in Fig. 2. As shown,

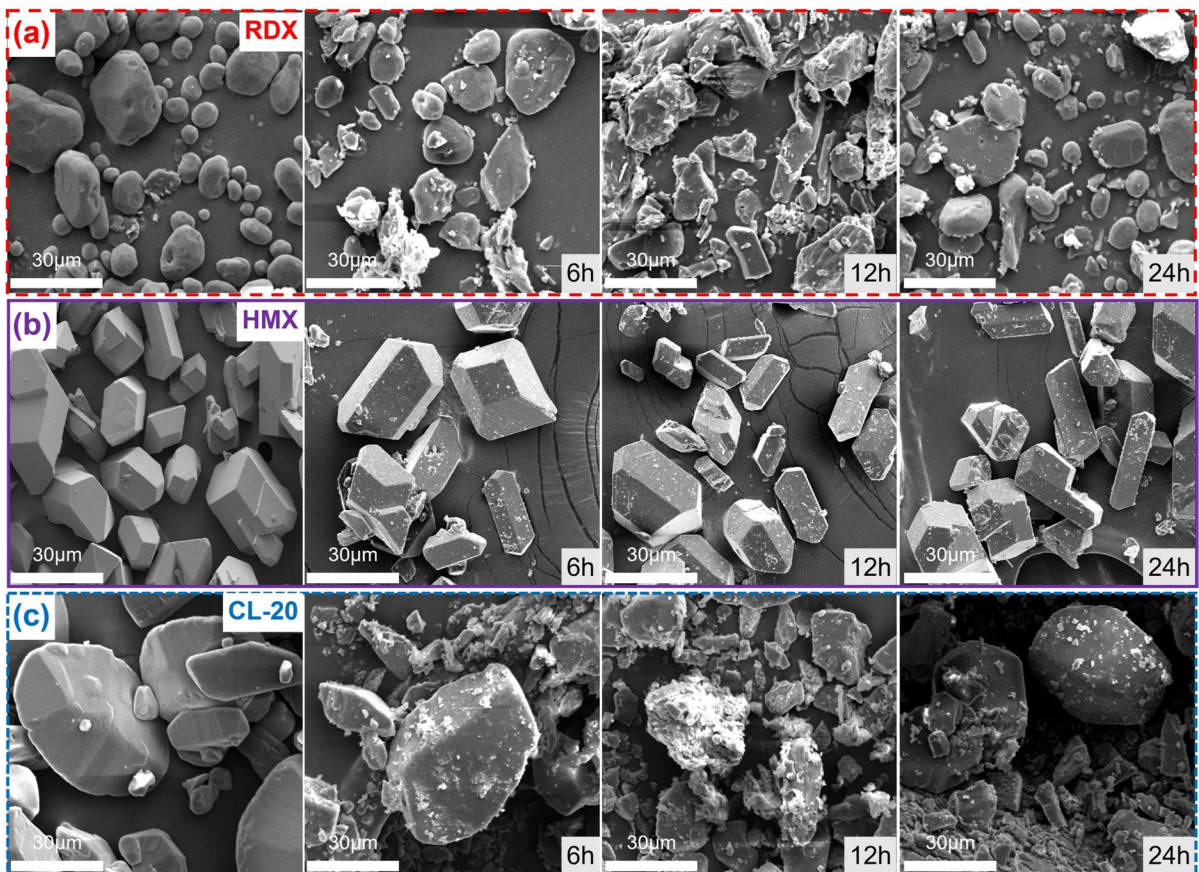


Fig. 2 The SEM images of RDX (a), HMX (b), CL-20 (c) and their corresponding CNFs@PDA coated energetic composites at different coating time (6 h, 12 h, 24 h)

the pristine crystals of RDX, HMX and CL-20 presented a smooth surface with morphologies of ellipsoidal surface, sharp-edge angle polyhedral and the average diameter was about 20 μm , 90 μm and 50 μm , respectively. After coated by CNFs@PDA, the surface morphology of energetic crystals was becoming relatively rougher because of the deposited polymeric CNFs@PDA composite fibers. This phenomenon exerted increase trend for the roughness on the surface of energetic crystal with the increase coating time from 6 to 24 h. That was to say, when the coating time of CNFs@PDA was short, that could not form a compact coating layer on the surface of energetic crystals. According to Fig. 2e–h, it can be noticed that the composites CNFs@PDA fibers was dispersed uniformly on the surface of HMX crystal. From Fig. 2i–l, it was found that deposited content of CNFs@PDA on surface of CL-20 crystal was gradually increasing following the increase coating time. As a consequence, the energetic crystal coated partially by CNFs@PDA fibers exhibited a coating structure and formed reasonably uniformly covering on the surface of crystals. In our previous study, it has demonstrated that a proper content of CNFs could deposit uniformly on the surface of energetic crystals, while slightly agglomeration occur when the addition content of CNFs was large. Therefore, in this work, it can be inferred that the dispersity of modified CNFs@PDA composites was further improved. The main reason could not only attribute to the similar core–shell structure of energetic composites where the crystal could provide enough attachment point for CNFs@PDA, but also result from the enhanced interaction between CNFs and energetic crystal due to the existence of PDA coating layer.

Composition and structure

To study the crystal structures stability of as-prepared energetic crystal composites modified by CNFs@PDA samples, XRD analysis was carried out as shown in Fig. 3a–c. As displayed, the characteristic diffraction maximums of RDX, HMX and CL-20 are indexed with JCPDS card no. 46-RDX: 1606, HMX: 45–1539, and CL-20: 50–2045, respectively. In terms of the CNFs@PDA coated energetic composites, the representative diffraction peaks of energetic crystals like RDX, HMX and CL-20 were maintained well without damaging, revealing that the inherent

structure of crystal has not been changed during the preparation process. However, it was found that the intensity of several diffraction peaks for the CNFs@PDA coated samples was varied compared to that of raw energetic crystals. For example, compared with raw RDX, RDX@(CNFs@PDA)_{1,3}-12 h decreased intensity at 2θ of 20.19°, 26.75°, 29.20°, and 32.13°, while that of RDX@(CNFs@PDA)-12 h increases in 17.58°, 25.18° and 29.12°; comparing to HMX, it can be found that the intensity of all diffraction peaks for HMX@(CNFs@PDA)_{1,3}-24 h was decreased dramatically; the similar variation of peak intensity could be noticed in CL-20@(CNFs@PDA)_{1,3}-12 h, while that of CL-20@(CNFs@PDA)-24 h increases in 12.58°, 12.81°, 13.83°, and 15.45°. In theory, the inherent orientation distribution characteristic of energetic crystals can generate various crystal surface signals during XRD analysis. Thus, these variations of peak intensity mentioned above could be attributed to the preferential orientation of crystals, which is extraordinarily widespread in the subject of crystallography. Particularly for polycrystalline energetic crystals HMX (e.g., α , β , γ , and σ) and CL-20 (e.g., α , β , γ , δ , and ϵ). After coated by CNFs@PDA, the preferential orientation of energetic crystals may probably result in the different intensity changes of diffraction peaks. Satisfactorily, as indicated, the optimized structure of β -HMX and ϵ -CL-20 was maintained favorably during the preparation process.

FT-IR spectroscopy was performed to study the organic functional groups of pristine energetic crystals and CNFs@PDA coated sample, as displayed in Fig. 3d–f. As can be seen, the absorption features of CNFs@PDA coated samples were not changed on the whole compared to that of pristine energetic crystals. However, a distinct phenomenon could be noticed that the spectral peaks locating at 3337 cm^{-1} were attributed to the –OH in CNFs@PDA, which became more evidently with the increase coating time and addition content of CNFs@PDA. With regard to other character absorption peaks marked in Fig. 3d–f), taking CL-20 and its corresponding composites as an example, the absorption peaks around 3044 cm^{-1} , 3017 cm^{-1} were resulted from the –CH₂ stretching vibration absorption peaks in cage or ring structure of CL-20 molecular; the bands at 1563 cm^{-1} and 1613 cm^{-1} indicated the (symmetry and asymmetry) stretching vibration absorption peak of –NO₂. Besides,

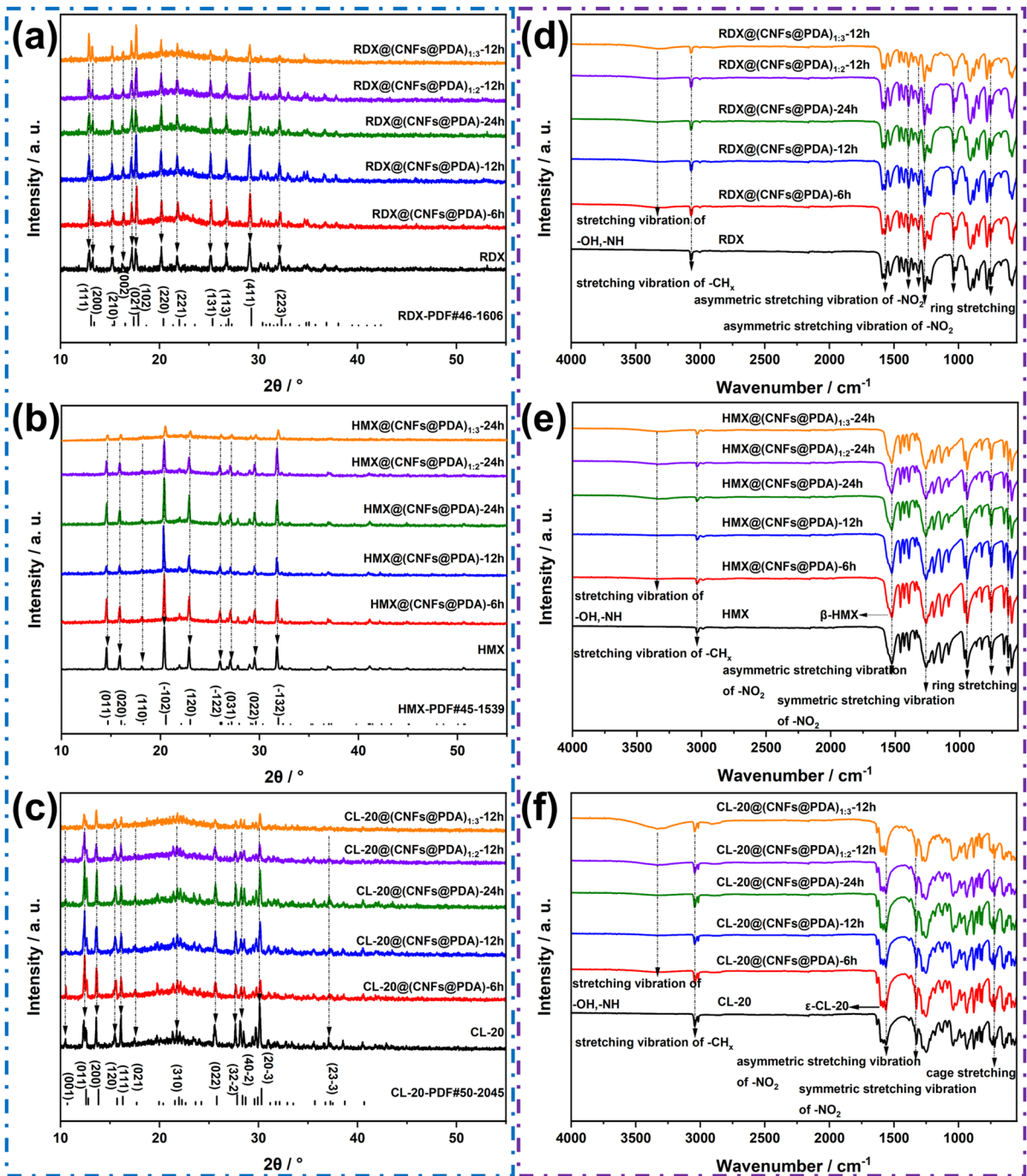


Fig. 3 The XRD patterns (a–c) and FT-IR spectra (d–f) of RDX, HMX, CL-20 and their corresponding composites

it should be noted that the intensity of absorption peak of CNFs@PDA samples was reduced slightly on the whole, as compared to that of pristine energetic crystal, and exerted a gradually decreased

trend with the increase coating time and addition content of CNFs@PDA, Therefore, these structural features confirmed the successfully wrapping of three energetic crystal by CNFs@PDA fibers.

Raman spectroscopy was another nondestructive, effective and fast characterization technique to detect both inorganic and organic materials, which provides a complementary function with FT-IR spectroscopy. Herein, it was performed for further demonstrating the successful modification of three energetic crystals. Raman spectroscopy features of RDX, HMX, CL-20 and CNFs@PDA coated samples were shown in Fig. 4a–c. As displayed, the bands located at the range of $100\text{--}736\text{ cm}^{-1}$, $748\text{--}1054\text{ cm}^{-1}$, $1148\text{--}1169\text{ cm}^{-1}$ were correspond to the ring or cage stretching, (symmetry and asymmetry) stretching vibration absorption peak of -NO_2 (-N-N), and the -CH_2 stretching vibration absorption peaks in cage

or ring structure of energetic crystals, respectively. Similar with FT-IR spectroscopy, the absorption peak intensity of Raman spectroscopy for CNFs@PDA coated products displayed a decreased trend with the increase coating time and addition content of CNFs@PDA. Moreover, after coated by CNFs@PDA, the Raman spectroscopy curves exhibited a certain of fluorescence, which was specifically expressed as the increasing gradient of curves. This result also demonstrated the successfully coating of three energetic crystal by CNFs@PDA.

To further study the composition and dispersity of the composites, the three-dimension (3D) of Raman mapping and the signal to baseline mapping images

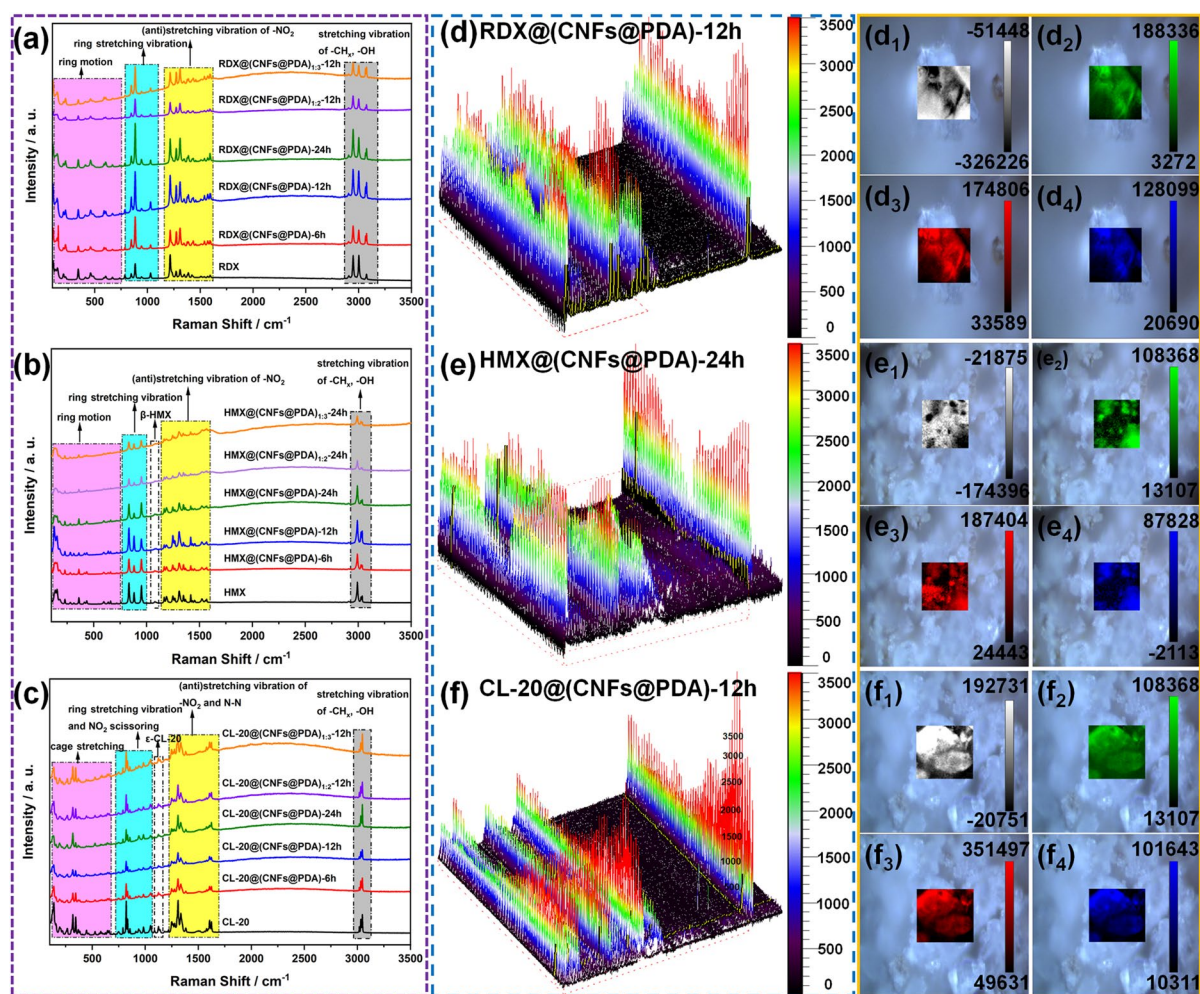


Fig. 4 The Raman spectra of RDX (a), HMX (b), CL-20 (c) and their corresponding composites, and the mapping images of 3D distribution of RDX@CNFs@PDA (d), HMX@

CNFs@PDA (e) CL-20@CNFs@PDA (f) and their corresponding signal baseline of groups (d₁–d₄), (e₁–e₄) and (f₁–f₄), respectively

are shown in Fig. 4d–f. It can be found that the compositions of composites were mainly divided into four groups. Taking HMX@(CNFs@PDA)-24 h as an example, the ring motion range of HMX (gray part) (Fig. 4e1), the ring vibrations stretching of HMX crystal molecule belongs to green part (Fig. 4e2), the anti-symmetric vibrations stretching of $-\text{NO}_2$ groups, which corresponded to red part (Fig. 4e3); while the $-\text{CH}_2$ vibrations was ascribed to blue part (Fig. 4e4). Thus, the above results of vibrational signal mapping images demonstrate the stable molecular structure of composites, and the 3D of distributions and signal to baseline mapping images also manifest a favorable dispersibility of the composites.

Thermal analysis

Thermal stability is generally assumed to be a significant performance for EMs. Herein, the DSC curves of RDX, HMX and CL-20, and their corresponding CNFs@PDA coated samples were performed at heating rate of $10\text{ }^\circ\text{C}\cdot\text{min}^{-1}$ in range of $100\text{--}350\text{ }^\circ\text{C}$, as shown in Fig. 5a. The corresponding thermal parameters were summarized in Table S1. As displayed, the exothermic peak temperature of RDX was gradually improved with the increase of coating time from 6 to 24 h, and transferred to a high temperature from 241.5 to $250.3\text{ }^\circ\text{C}$. It was worth noting that the increased addition content for CNFs@PDA in composites system seemed to not further improve the exothermic peak temperature, while became decreasing with the increased addition content. For example, the exothermic peak temperature of $\text{RDX}(\text{CNFs@PDA})_{1:3}$ was decreased to $245.1\text{ }^\circ\text{C}$. As for the endothermic peak temperature, it was just improved slightly, which seemed to be not influenced by the coating layer of CNFs@PDA. The similar variation phenomenon of exothermic and endothermic peak temperature could be found for HMX and its corresponding CNFs@PDA coated samples. However, the endothermic peak temperature of $\text{HMX}(\text{CNFs@PDA})_{1:3}$ ($205.1\text{ }^\circ\text{C}$) was also much larger than that of HMX ($184.1\text{ }^\circ\text{C}$), which indicated that the polymorph stability of $\text{HMX}(\text{CNFs@PDA})$ composites was improved. With regard to CL-20, the exothermic and endothermic peak temperature of $\text{CL-20}(\text{CNFs@PDA})$ composite exerted an increased trend with the increased coating time and addition content of CNFs@PDA. Therein, the exothermic peak temperature was

increased from 239.1 to $246.7\text{ }^\circ\text{C}$, while the endothermic peak temperature was increased from 162.7 to $182.2\text{ }^\circ\text{C}$. On another hand, the heat release of composites decreased due to the addition of inert materials. For instance, the value of heat release for RDX, HMX and CL-20 was $1418\text{ J}\cdot\text{g}^{-1}$, $1643\text{ J}\cdot\text{g}^{-1}$, and $1966\text{ J}\cdot\text{g}^{-1}$, while that of $\text{RDX}(\text{CNFs@PDA})_{1:3}$, $\text{HMX}(\text{CNFs@PDA})_{1:3}$ and $\text{CL-20X}(\text{CNFs@PDA})_{1:3}$ was $746.8\text{ J}\cdot\text{g}^{-1}$, $868.4\text{ J}\cdot\text{g}^{-1}$ and $970\text{ J}\cdot\text{g}^{-1}$, respectively. Therefore, the mentioned above results demonstrated that a proper coating time and suitable addition content of CNFs@PDA can remarkably improve the polymorph stability of HMX and CL-20 and the thermal decomposition stability of three nitramine explosives.

TG analysis was further conducted to study the thermal decomposition weight loss process of RDX, HMX and CL-20, and their corresponding CNFs@PDA coated samples, as shown in Fig. 5b. The corresponding thermal parameters were displayed in Table S2. It can be found that the step of weight loss was gradually divided into two steps with the increasing coating time and addition content of CNFs@PDA. Taking $\text{RDX}(\text{CNFs@PDA})_{1:3}$ as an example, the first step of weight loss could attribute to the decomposition of RDX crystals, while the second one should ascribe to the decomposition of CNFs@PDA. This similar phenomenon could also be noticed in HMX, CL-20 and their corresponding composites, especially for $\text{HMX}(\text{CNFs@PDA})_{1:3}$ and $\text{RDX}(\text{CNFs@PDA})_{1:3}$. Therein, the RDX, HMX and CL-20 stated to decompose early from about $225\text{ }^\circ\text{C}$, $278\text{ }^\circ\text{C}$ and $240\text{ }^\circ\text{C}$, respectively, while that of CNFs@PDA became decompose at approximately $350\text{ }^\circ\text{C}$. The above-mentioned results manifested that multistep weight loss behavior was more evidently with the increase addition of CNFs@PDA, whereas the mass of composites was seemingly to be increased compared with other samples. The main reason could be ascribed to the exist of large content of CNFs@PDA particle in composites, whose decomposition behavior was not entirely and remain in reaction products. Therefore, based on the mentioned above results of DSC, TG analysis, it can be obtained that these nitramine explosive crystals modified by CNFs@PDA revealed different thermal decomposition performance, including the improved thermal stability, polymorph stability, step-by-step of decomposition weight lost behavior. Besides, it also demonstrated

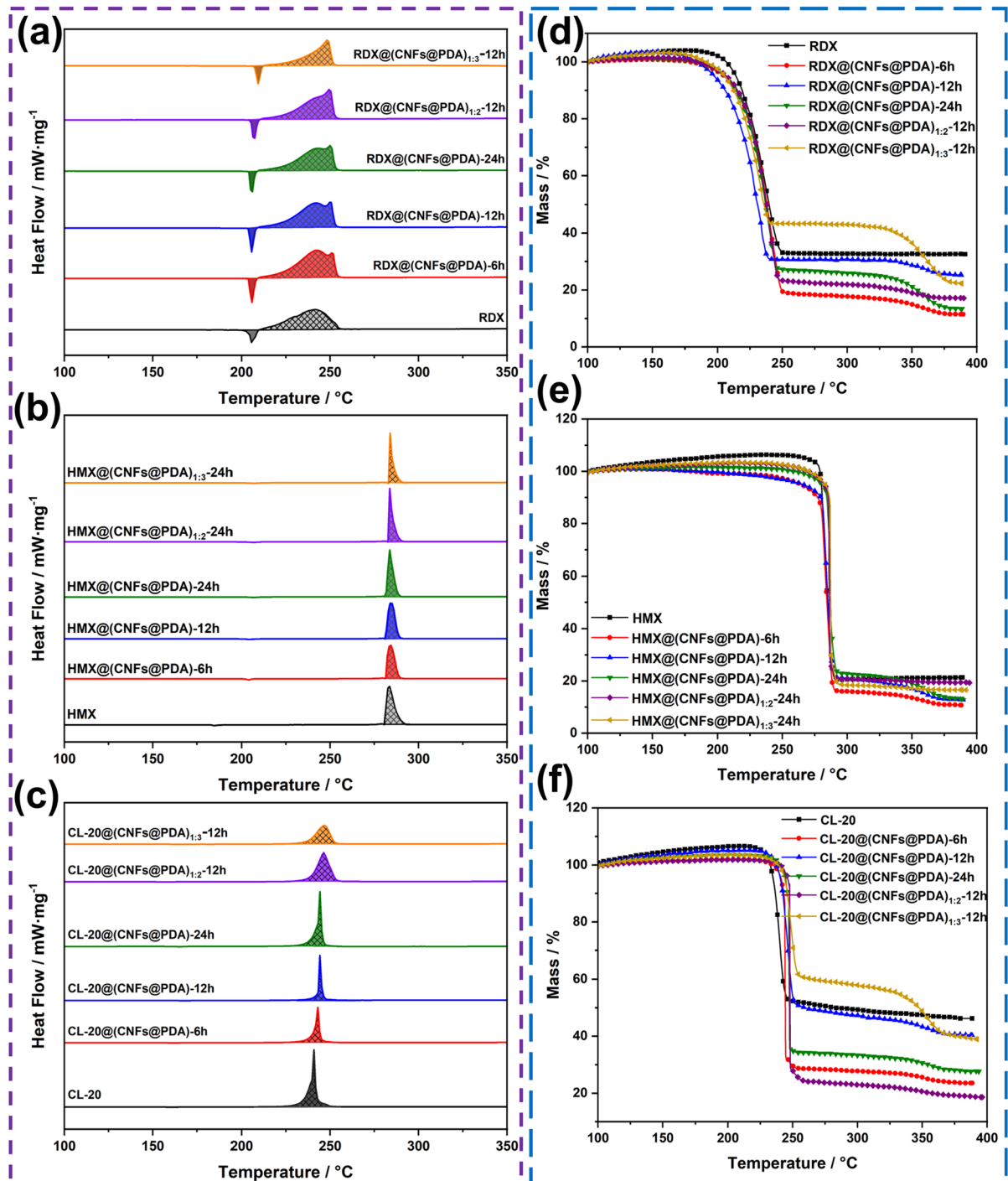


Fig. 5 The DSC curves (a–c) and TG analysis (d–f) of RDX, HMX, CL-20 and their corresponding composites coated by CNFs@PDA

that energetic crystals modified with a proper content of CNFs@PDA composites is necessary and need to be controlled.

Sensitivity performance

In Fig. 6, the sensitivity tests including impact, friction and electrostatic spark were performed to evaluate the safety performance RDX, HMX and CL-20, and their corresponding CNFs@PDA coated

samples. As displayed, after coated by CNFs@PDA, the obtained composites presented much lower sensitivity compared with neat energetic crystals. It was found that the sensitivity exerted decreased trend with the increase coating time and addition content of CNFs@PDA. For instance, in Fig. 6a, the value of H_{50} for RDX was 31.1 cm, after coated by CNFs@PDA with coating time about 6 h, 12 h and 24 h, that of H_{50} was increased to 34.5 cm, 38.8 cm, and 41.6 cm. In addition, with the increase addition of

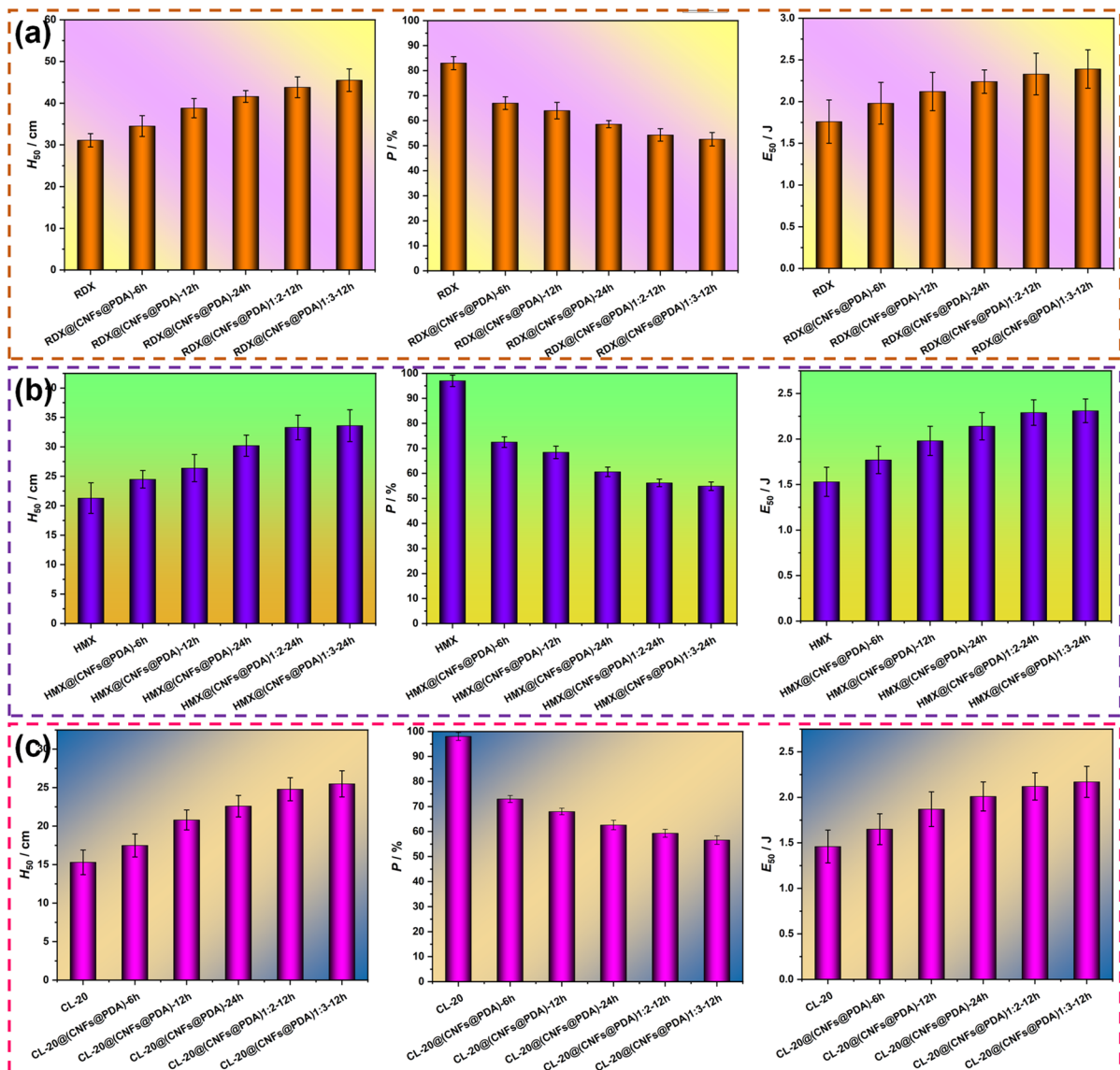


Fig. 6 The impact, friction and electrostatic spark sensitivity of pristine RDX (a), HMX (b) and CL-20 (c), and their corresponding (CNFs@PDA) coated composites

CNFs@PDA content, that of H_{50} for RDX@(CNFs@PDA)_{1:2} and RDX@(CNFs@PDA)_{1:3} was further increased to 43.8 cm and 45.5 cm. The similar variation regular for sensitivity could be found in HMX and CL-20, and their corresponding CNFs@PDA coated samples as well. It indicated that the formation of CNFs@PDA shell layer could effectively desensitize these energetic crystals and grants the composites with favorable insensitivity character. Besides, both of the coating time and the addition content of CNFs@PDA has influence on the sensitivity behavior.

To further analysis the desensitization mechanism of the CNFs@PDA coated samples, Fig. 7 proposal the probable mechanism of reduction sensitivity. In general, the generation of hot spots is the dominating cause controlling the explosion of explosive crystals, and it occurs when going through these processes of production, growth and diffusion, once suffering from some extrinsic stimulation. Herein, in this study,

the results of sensitivity variations demonstrated that the CNFs@PDA coating layer could effectively improve the insensitivity of energetic crystals, which can be explained from the following aspects. Firstly, when the CNFs@PDA particles were coated on the edges or corners of HMX and CL-20 crystals, the hot spots could be reduced through covering the margins and nooks of HMX and CL-20 after coated by CNFs@PDA, as shown in Fig. 7a. That was to say, the CNFs@PDA coating layer played a function role of lubrication. On another hand, the quite thick shell layer of deposited CNFs@PDA on the surface of crystals could hinder the diffusion of exothermic stimuli. Secondly, the various morphology of energetic crystals also form different thickness of PDA shell layer, leading to partial stimulation touching the core after experiencing the buffer layer of CNFs@PDA. While CNFs act as a buffer system to isolate the potential hot spots and prevent its incorporation

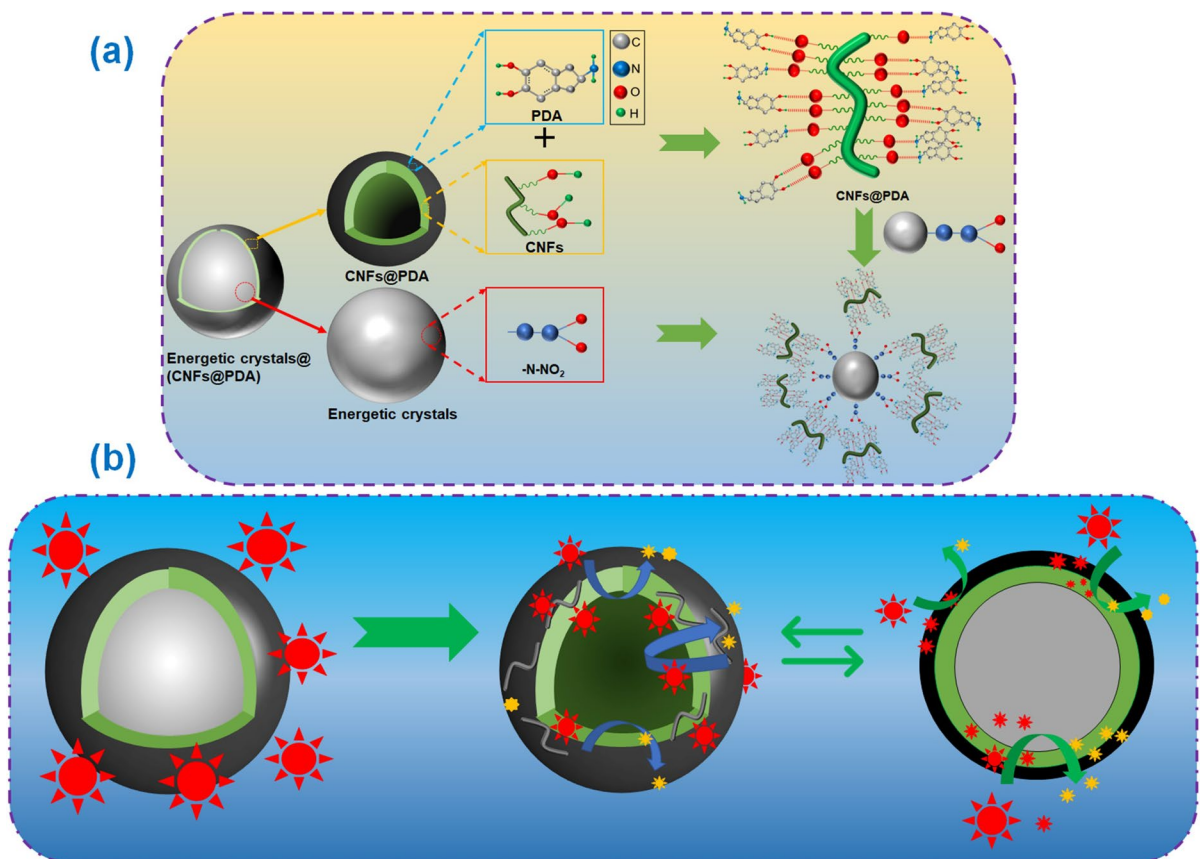


Fig. 7 The proposal mechanism of CNFs@PDA coating and desensitization for energetic crystals

and fast development. For example, the homogeneous distribution of CNFs@PDA on the surface of RDX was able to reduce the generation possibility of hot spots. Finally, the existence of CNFs@PDA could decrease the squeeze, cut, or rub among crystals to weaken the generation possibility of hot spots. Moreover, the formation of hydrogen bond between crystals and CNFs@PDA could absorb the energy of exothermic stimuli and release them, as displayed in Fig. 7b. Thus, the form of CNFs@PDA layer can be regarded as a safe cushion to liberate extrinsic stimuli and act as the earliest assailed to disperse the exterior stimulation from the surroundings, thereby tremendously lowering the possibility of hot spot production and decreasing the sensitivity of CNFs@PDA coated energetic crystals.

Conclusion

In summary, this study constructed a series of CNFs@PDA coated energetic composites via a simple and safe in-suit self-polymerization method and water suspension method. The obtained composites exerted stable structure and composition without crystal transfer for HMX and CL-20. It was found that the CNFs@PDA coating layer was deposit uniformly on the surface of energetic crystals. The thermal stability was improved remarkably with a proper coating time and addition of CNFs@PDA content. The exist of CNFs@PDA coating layer granted the composites with different process of weight loss compared with neat crystals. Meanwhile, the sensitivity of the obtained samples exerted a decreasing trend with the increased coating time and addition content of CNFs@PDA, and a probable desensitization mechanism of coating shell lubrication release energy was proposal. Hence, this fabrication strategy and properties of energetic crystal@(CNFs@PDA) composites may offer a promising application of CNFs and PDA in high-strength and high-strength propellants.

Acknowledgments This study thanks Dr. Wang Binbing and Prof. Xu Bin for their experimental help and technical support. Thanks to the analysis and testing center of Nanjing university of science and technology for their experimental help and technical support. This study thanks to the supporting of Jiangsu Funding Program for Excellent Postdoctoral Talent.

Author contributions LC and DM are co-first authors of the article. LC: Data curation, Methodology, Writing-Original draft preparation. JZ: Second corresponding author, Conceptualization, Raw materials provider, Writing-Reviewing and Editing, Funding acquisition. DM: Data curation. XC: Writing-Editing. FN: Supply for the experimental platform, funding provider, Writing-Editing. XL: Writing-Reviewing and Editing. WH: First corresponding author, Conceptualization, Raw materials provider, Writing-Reviewing and Editing, Funding acquisition.

Funding This work was supported by the Jiangsu Funding Program for Excellent Postdoctoral Talent.

Data availability Data and materials can be obtained on request from authors by email.

Declarations

Conflict of interest We declare that this manuscript have no any commercial or associative interest that represents a conflict of interest.

Ethical approval Not applicable.

Consent for publication All the authors listed have approved the enclosed manuscript for publication.

References

- Aduev BP, Nurmukhametov DR, Liskov IY, Zvekov AA (2021) RDX-Al and PETN-Al composites' glow spectral kinetics at the explosion initiated with laser pulse. *Combust Flame* 223:376–381
- Cady HH, Larson AC, Cromer DT (1963) The crystal structure of α -HMX and a refinement of the structure of β -HMX. *Acta Crystallogr A* 16:617–623
- Chauhan BS, Thakur A, Soni PK, Kumar M (2021) Recrystallization of CL-20 to ϵ -polymorphic form. In: IOP conference series materials science and engineering, pp 1033
- Chen L, Cao X, Chen Y, Li Q, Wang Y, Wang X, Qin Y, Cao X, Liu J, Shao Z et al (2021a) Biomimetic-inspired one-step strategy for improvement of interfacial interactions in cellulose nanofibers by modification of the surface of nitramine explosives. *Langmuir* 37:8486–8497
- Chen L, Cao X, Gao J, He W, Liu J, Wang Y, Zhou X, Shen J, Wang B, He Y et al (2021b) Nitrated bacterial cellulose-based energetic nanocomposites as propellants and explosives for military applications. *ACS Appl Nano Mater* 4:1906–1915
- Chen L, Liu J, He W (2021c) Bio-inspired fabrication of energetic crystals@cellulose nanofibers core-shell composites with improved stability and reduced sensitivity. *Compos Commun* 27:100868
- De France K, Zeng Z, Wu T, Nyström G (2021) Functional materials from nanocellulose: utilizing structure-property

- relationships in bottom-up fabrication. *Adv Mater* 33:e2000657
- Doukkali M, Gauthier E, Patel RB, Stepanov V, Hadim H (2017) Modifying the wettability of nitramine explosives using anionic, cationic and nonionic surfactants. *Propellants Explos Pyrotech* 42:1185–1190
- Dreyer DR, Miller DJ, Freeman BD, Paul DR, Bielawski CW (2013) Perspectives on poly(dopamine). *Chem Sci* 4:3796
- Gong F, Zhang J, Ding L, Yang Z, Liu X (2017) Mussel-inspired coating of energetic crystals: a compact core-shell structure with highly enhanced thermal stability. *Chem Eng J* 309:140–150
- Guillevic M, Pichot V, Cooper J, Coquerel G, Borne L, Spitzer D (2020) Optimization of an antisolvent method for RDX recrystallization: influence on particle size and internal defects. *Cryst Growth Des* 20:130–138
- He G, Yang Z, Pan L, Zhang J, Liu S, Yan Q-L (2017) Bioinspired interfacial reinforcement of polymer-based energetic composites with a high loading of solid explosive crystals. *J Mater Chem Mater Energy Sustain* 5:13499–13510
- Huang D, Wu M, Wang C, Kuga S, Huang Y (2020) Effect of partial dehydration on freeze-drying of aqueous nanocellulose suspension. *ACS Sustain Chem Eng* 8:11389–11395
- Huang B, Xue Z, Fu X, Yan Q-L (2021) Advanced crystalline energetic materials modified by coating/intercalation techniques. *Chem Eng J* 417:128044
- Jia X, Wang J, Hou C, Tan Y, Zhang Y (2018) Effective insensitiveness of melamine urea-formaldehyde resin via interfacial polymerization on nitramine explosives. *Nanoscale Res Lett* 13:1–12
- Jia X, Cao Q, Guo W, Li C, Shen J, Geng X, Wang J, Hou C (2019) Synthesis, thermolysis, and solid spherical of RDX/PMMA energetic composite materials. *J Mater Sci Mater Electron* 30:20166–20173
- Lee H, Dellatore SM, Miller WM, Messersmith PB (2007) Mussel-inspired surface chemistry for multifunctional coatings. *Science* 318:426–430
- Lin C, Gong F, Yang Z, Pan L, Liu S, Li J, Guo S (2018) Bioinspired fabrication of core@shell structured TATB/polydopamine microparticles via in situ polymerization with tunable mechanical properties. *Polym Test* 68:126–134
- Lin C, Gong F, Yang Z, Zhao X, Li Y, Zeng C, Li J, Guo S (2019) Core-shell structured HMX@polydopamine energetic microspheres: synergistically enhanced mechanical, thermal, and safety performances. *Polymers* 11:568
- Liu Y, Ai K, Lu L (2014) Polydopamine and its derivative materials: synthesis and promising applications in energy, environmental, and biomedical fields. *Chem Rev* 114:5057–5115
- Liu Y, Xu J, Huang S, Li S, Wang Z, Li J, Jia J, Huang H (2019) Microstructure and performance of octahydro-1,3,5,7-tetranitro-1,3,5,7-tetrazocine (HMX) crystal clusters obtained by the solvation-desolvation process. *J Energ Mater* 37:282–292
- Maerten C, Garnier T, Lupattelli P, Chau NTT, Schaaf P, Pierry L, Boulmedais F (2015) Morphogen electrochemically triggered self-construction of polymeric films based on mussel-inspired chemistry. *Langmuir* 31:13385–13393
- Mao X, Jiang L, Zhu C, Wang X (2018) Effects of aluminum powder on ignition performance of RDX, HMX, and CL-20 explosives. *Adv Mater Sci Eng* 2018:1–8
- Shen F, Lv P, Sun C, Zhang R, Pang S (2014) The Crystal structure and morphology of 2,4,6,8,10,12-Hexanitro-2,4,6,8,10,12-hexaazaisowurtzitane (CL-20) *p*-Xylene solvate: a joint experimental and simulation study. *Molecules* 19:18574–18589
- Shen J, Liu Z, Xu B, Liang H, Zhu Y, Liao X, Wang Z (2019) Influence of carbon nanofibers on thermal and mechanical properties of NC-TEGDN-RDX triple-base gun propellants. *Propellants Explos Pyrotech* 44:355–361
- Shen J, Liu Z, Xu B, Chen F, Zhu Y, Fu Y, Kline DJ, Liao X, Wang Z (2020) Tuning the thermal, mechanical, and combustion properties of NC-TEGDN-RDX propellants via incorporation of graphene nanoplates. *J Energ Mater* 38:326–335
- Shu YJ, Wu ZK, Liu N, Ding XY, Lu YY (2015) Crystal control and cocrystal formation: important route of modification research of energetic materials. *Chin J Explos Propellants*
- Sinditskii VP, Yudin NV, Fedorchenko SI, Egorshv VY, Kostin NA, Gezalyan LV, Zhang J-G (2020) Thermal decomposition behavior of CL-20 co-crystals. *Thermochim Acta* 691:178703
- Song X, Wang Y, Zhao S, Li F (2018) Mechanochemical fabrication and properties of CL-20/RDX nano co/mixed crystals. *RSC Adv* 8:34126–34135
- Wang Z, Guo X, Wu F, Yan T (2016) Preparation of HMX/TATB composite particles using a mechanochemical approach. *Propellants Explos Pyrotech* 41:327–333
- Wang S, An C, Wang J, Ye B (2018) Reduce the sensitivity of CL-20 by improving thermal conductivity through carbon nanomaterials. *Nanoscale Res Lett* 13:1–8
- Wang G, Xiang J, Lin J, Xiang L, Chen S, Yan B, Fan H, Zhang S, Shi X (2020a) Sustainable advanced Fenton-like catalysts based on mussel-inspired magnetic cellulose nanocomposites to effectively remove organic dyes and antibiotics. *ACS Appl Mater Interfaces* 12:51952–51959
- Wang Y, Yang H, Han J, Gao K (2020b) Effect of DGTN content on mechanical and thermal properties of modified single-base gun propellant containing NQ and RDX. *Propellants Explos Pyrotech* 45:128–135
- Xie W, Zhao Y, Zhang W, Liu Y, Fan X, Wang B, He W, Yan QL (2018) Sensitivity and stability improvements of NEPE propellants by inclusion of FOX-7. *Propellants Explos Pyrotech* 43:308–314
- Yang Z, Ding L, Wu P, Liu Y, Nie F, Huang F (2015) Fabrication of RDX, HMX and CL-20 based microcapsules via in situ polymerization of melamine-formaldehyde resins with reduced sensitivity. *Chem Eng J* 268:60–66
- Ye B, An C, Zhang Y, Song C, Geng X, Wang J (2018) One-step ball milling preparation of nanoscale CL-20/graphene oxide for significantly reduced particle size and sensitivity. *Nanoscale Res Lett* 13:1–8
- Yuan LU, Xiao-Qing WU (2011) Research of surface coating of explosive particles. *Guangzhou Chemical Industry*
- Zeng C, Yang Z, Wen Y, He W, Zhang J, Wang J, Huang C, Gong F (2021) Performance optimization of core-shell HMX@Al(GAP) aluminized explosives. *Chem Eng J* 407:126360

- Zhang Y, Liu C, Lv Y, Zhou Z, Wang F, Shao Z, Zuo Y, Wei X (2016) Preparation and characteristic of modified double-base propellant modified with cellulose nanofibers. *Integr Ferroelectr* 171:115–123
- Zhang X-Q, Chen X-R, Kaliamurthi S, Selvaraj G, Ji G-F, Wei D-Q (2018) Initial decomposition of the co-crystal of CL-20/TNT: sensitivity decrease under shock loading. *J Phys Chem C* 122:24270–24278
- Zhang S, Kou K, Zhang J, Jia Q, Xu Y (2019a) Compact energetic crystals@ urea-formaldehyde resin micro-composites with evident insensitivity. *Compos Commun* 15:103–107
- Zhang Y-J, Bai Y, Li J-Z, Fu X-L, Yang Y-J, Tang Q-F (2019b) Energetic nitrocellulose coating: effective way to decrease sensitivity and modify surface property of HMX particles. *J Energ Mater* 37:212–221
- Zhou X, Zhu Y, Cheng Z, Ke X, Shi K, Zhang K (2019) Preparation of cyclotrimethylenetrinitramine-copper oxide core-shell particles and their thermal decomposition kinetics. *Propellants Explos Pyrotech* 44:1368–1374

Publisher's Note Springer Nature remains neutral with regard to jurisdictional claims in published maps and institutional affiliations.

Springer Nature or its licensor (e.g. a society or other partner) holds exclusive rights to this article under a publishing agreement with the author(s) or other rightsholder(s); author self-archiving of the accepted manuscript version of this article is solely governed by the terms of such publishing agreement and applicable law.